Grain Boundary Assemblies in Dynamically-Recrystallized Austenitic Stainless Steel

Marina Tikhonova *, Pavel Dolzhenko, Rustam Kaibyshev and Andrey Belyakov

Laboratory of Mechanical Properties of Nanostructured Materials and Superalloys, Belgorod State University, Pobeda 85, Belgorod 308015, Russia; dolzhenko.p@yandex.ru (P.D.); rustam_kaibyshev@bsu.edu.ru (R.K.); belyakov@bsu.edu.ru (A.B.)

* Correspondence: tikhonova@bsu.edu.ru; Tel.: +7-4722-585457

Abstract: The grain boundary misorientation distributions associated with the development of dynamic recrystallization were studied in a high-nitrogen austenitic stainless steel subjected to hot working. Under conditions of discontinuous dynamic recrystallization, the relationships between the grain or subgrain sizes and flow stresses can be expressed by power law functions with different grain/subgrain size exponents of about -0.76 (for grain size) or -1.0 (for subgrain size). Therefore, the mean grain size being much larger than the subgrain size under conditions of low flow stress gradually approaches the size of the subgrains with an increase in the flow stress. These dependencies lead to the fraction of high-angle boundaries being a function of the flow stress. Namely, the fraction of ordinary high-angle boundaries in dynamically-recrystallized structures decreases with a decrease in the flow stress. On the other hand, the fraction of special boundaries, which are associated with annealing twins, progressively increases with a decrease of the flow stress.

Keywords: dynamic recrystallization; austenitic stainless steel; grain boundary engineering; hot working

1. Introduction

Dynamic recrystallization (DRX) is a very effective tool to obtain a desirable microstructure in various metallic materials [1–4]. The DRX microstructures depend sensitively on the deformation conditions, i.e., temperature (T) and strain rate ($\dot{\varepsilon}$), which are commonly represented by a temperature-compensated strain rate, the Zener-Hollomon parameter ($Z = \dot{\varepsilon} \exp Q/RT$, where Q and R are the activation energy and the universal gas constant, respectively) [5,6]. One of the most important structural parameters is grain size, which significantly affects properties of metals and alloys; especially, their mechanical/deformation behavior [7]. The grain size in DRX microstructures can be controlled by deformation conditions, e.g., it increases with an increase in the deformation temperature and/or a decrease in the strain rate [8,9]. The flow stress during hot deformation of various metals and alloys also depends on the deformation conditions and can be expressed by a power law function of Z. Therefore, a power law generally holds between the flow stress and the DRX grain size with a grain size exponent of about -0.7 for hot working conditions [10–12].

In contrast to the size of DRX grains, which has been a subject of numerous investigations along with the fraction and distribution of DRX grains [2], the grain boundary character distributions that develop during DRX have not been studied in sufficient details. The DRX mechanism that operates under hot working conditions involves a local bulging of a grain boundary portion leading to the development of a DRX nucleus. Then, the DRX nucleus grows out, consuming the work-hardened surroundings until it impinges with other growing DRX grains, or the driving force for the DRX grain growth drops below a critical value due to the increase in the deformation stored energy in

the growing DRX grain during deformation. Therefore, there are several grain types in the DRX microstructure, including DRX nuclei, growing DRX grains, and work-hardened grains. The latter ones involve a number of low-angle dislocation subboundaries. Moreover, annealing twins may appear in the growing DRX grains as a result of a growth accident of a migration boundary in metals and alloys with low stacking fault energy (SFE) [12,13], since the growth of DRX grains is associated with the migration of their boundaries. The fraction and density of twin-related boundaries, which are characterized by special coincident site lattices ($\Sigma 3^n$ CSL), have been frequently studied for static recrystallization and grain growth [14–16]. It has been suggested that both the fraction and density of $\Sigma 3^n$ CSL boundaries depend on a relative change in the grain size and, thus, can be expressed by functions of the size ratio of an instant grain (after recrystallization or grain growth) to the initial one (just before recrystallization/grain growth) [17–19]. A similar relationship between the fraction of $\Sigma 3^n$ CSL boundaries and grain size ratio has been obtained for continuous post-dynamic recrystallization of an austenitic stainless steel [20]. On the other hand, the development of $\Sigma 3^n$ CSL boundaries in low-SFE materials during conventional discontinuous DRX under hot working conditions has not been clarified.

The aim of the present paper is to study the grain boundary assemblies that develop during discontinuous DRX in an austenitic stainless steel. It places particular emphasis on quantitative relationships between the grain boundary character distributions and hot working conditions. A high-nitrogen chromium-nickel stainless steel was selected in the present study as a representative of advanced structural steels designated for crucial engineering applications sustainable against loading under low-temperature conditions.

2. Materials and Methods

A high-nitrogen austenitic stainless steel, 0.025%C–22%Cr–10.2%Ni–0.36%N–6.2%Mn–0.34%Si–1.9%Mo–0.003%S–0.005%P and the balance Fe (all in wt %), was cast at the Central Research Institute for Machine-Building Technology, Moscow, Russia. The steel was solution annealed and hot rolled at a temperature of 1373 K. The average grain size was approximately 420 μm. Rectangular samples with initial dimensions of 10 mm × 12 mm × 15 mm were machined for compression tests, which were carried out using an Instron 300LX testing machine (Instron Ltd., Norwood, MA, USA) equipped with a three-sectioned high-temperature furnace (Instron Ltd., Norwood, MA, USA). A powder of boron nitride was used as a lubricant to minimize the friction between the specimen and anvil. The specimens were compressed at temperatures of 1073 K to 1348 K, and strain rates of 10^{-4} s^{-1} to 10^{-2} s^{-1}, and then immediately quenched by water jet while the deformation was ceased (the quench delay was 1–2 s).

The structural investigations were carried out on the sample sections parallel to the compression axis using a Nova Nano SEM 450 scanning electron microscope (FEI Corporation, Hillsboro, OR, USA) equipped with an electron backscatter diffraction (EBSD) analyzer (Oxford Instruments, Oxfordshire, UK) incorporating an orientation imaging microscopy (OIM) system (Oxford Instruments, Oxfordshire, UK). The OIM images were subjected to clean-up procedures, setting a minimal confidence index of 0.1. The grain size (D) was measured as an average distance between ordinary high-angle boundaries (HABs), i.e., those with misorientations of $\theta \geq 15°$, excepting the $\Sigma 3^n$ CSL boundaries, along and crosswise to the compression axis. In the case of uncompleted DRX, the DRX grains were distinguished from non-recrystallized portions by means of kernel average misorientation, assuming that the kernel average misorientation within DRX portions did not exceed $1°$. The subgrain size (d) was measured as an average distance between subboundaries with misorientations of $1° < \theta < 15°$.

3. Results

3.1. Stress-Strain Curves

Figure 1 shows a series of true stress-strain curves obtained during hot isothermal compressions at different temperatures and strain rates. Most of the curves exhibit typical DRX behavior with a peak flow stress followed by a steady state deformation behavior [3,21]. Note here that an apparent increase in the flow stress at large strains is associated with a growing contribution from contact friction stresses. The flow stresses vary with the deformation temperature and strain rate. The flow stresses decrease with an increase in the deformation temperature (Figure 1a) or with a decrease in the strain rate (Figure 1b). The peak flow stress increases by 30%–40% with a ten-fold increase in the strain rate, if the temperature is a constant. A decrease in the deformation temperature results in the peak flow stress occurring at larger strain that is much similar to other studies on DRX at hot working conditions [1,2,5,22]. This suggests, therefore, that the DRX kinetics slow down as the deformation temperature decreases. At relatively low deformation temperatures below 1173 K, the steady state deformation behavior can hardly be distinguished through the flow curves in Figure 1a.
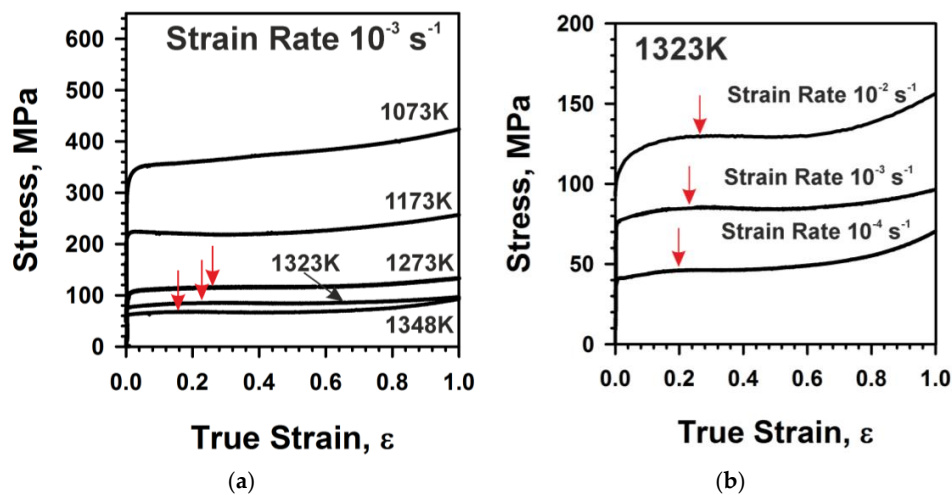
Figure 1. The true stress-true strain curves of the high nitrogen austenitic stainless steel under various deformation conditions, i.e., at strain rate of 10^{-3} s^{-1} (**a**) and at a temperature of 1323 K. (**b**) The red arrows indicate the peak stress associated with DRX.

3.2. Deformation Microstructures

Typical deformation microstructures that developed during hot isothermal compressions at temperatures of 1073–1323 K are shown in Figure 2. The deformation microstructures are characterized by pancake-shaped original grains, which are separated from each other by thin chains of ultrafine DRX grains, after compression at 1073 K (Figure 2). The fraction of DRX grains increases with the increase in the deformation temperature. The coarse remnants of the original grains are surrounded by numerous DRX grains in the sample compressed at 1173 K (Figure 2). The development of DRX grains readily takes place along the original grain boundaries [1,3,10]. Therefore, so-called necklace microstructures are evolved in the partially-recrystallized samples in Figure 2. It is clearly seen in Figure 2 that uniform fine-grained microstructures are completely developed in the samples processed at temperatures of $T \geq 1273$ K. As it could be expected, these fine-grained DRX microstructures involve various boundaries, including rather large fractions of low-angle subboundaries and twin-related $\Sigma3^n$ CSL boundaries (some of them are indicated by arrows in Figure 2) besides ordinary high-angle grain boundaries.
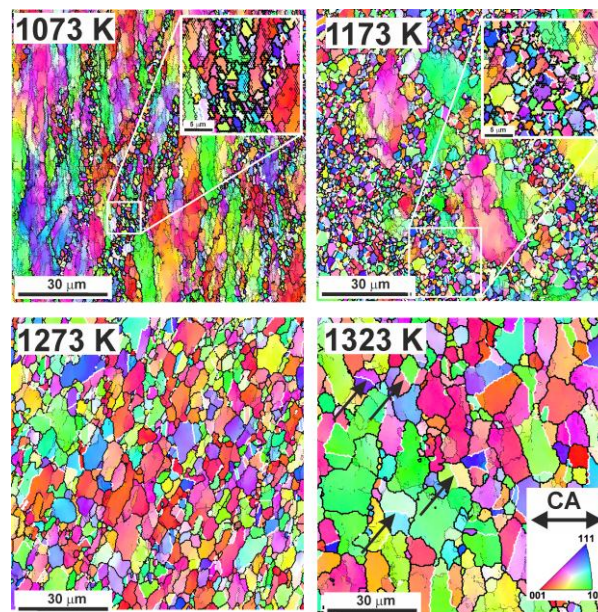
Figure 2. Typical microstructures that evolved in the high-nitrogen austenitic stainless steel during compression to a strain of 1.2 at 1073–1323 K and a strain rate of 10^{-3} s^{-1}. The thin and thick lines correspond to the subgrain and grain boundaries, respectively. The white line corresponds to CSL $\Sigma3^n$ boundaries. The colors reflect the inverse pole figures for the compression axis (CA). The arrows indicate some typical twins by growth accident.

The presence of large fractions of non-recrystallized portions in the DRX necklace microstructures evolved at 1073–1173 K results in bimodal grain size distributions (Figure 3). The fraction of large non-recrystallized grains comprises 0.74 at 1073 K. Correspondingly, the fraction of DRX grains at this temperature is 0.26. An increase in the deformation temperature leads to an increase in the DRX fraction. The peak of the grain size distribution against the large grain sizes, which corresponds to non-recrystallized remnants of the original grains, decreases and spreads out towards smaller sizes. At 1173 K, the fraction of recrystallized portions increases to 0.5.
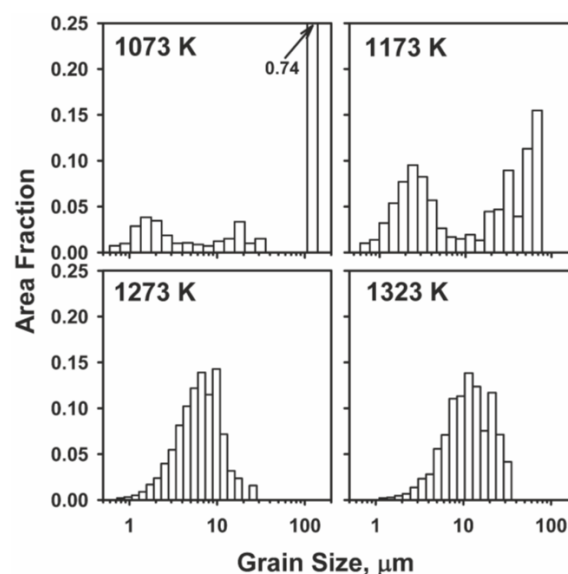
Figure 3. Grain size distributions that evolved in the high-nitrogen austenitic stainless steel during compression to a strain of 1.2 at the indicated temperatures and a strain rate of 10^{-3} s^{-1}.

Fully-recrystallized microstructures develop in the samples compressed at 1273–1348 K. The corresponding grain size distributions are characterized by a single peak against grain sizes ranging from 1–2 μm to 10–40 μm, depending on the deformation temperature (Figure 3).

3.3. DRX Grains and Their Boundaries

Let us consider the DRX grain evolution during compressions at different temperatures and strain rates in more detail. The temperature and strain rate effects on the average grain and subgrain sizes are shown in Figure 4. Note here that the non-recrystallized portions were omitted while considering the DRX grains/subgrains and their boundaries in the partially-recrystallized microstructures. The grain/subgrain sizes exhibit apparently weak temperature and strain rate dependencies at relatively low temperatures. The average DRX grain and subgrain sizes fall in almost the same range of 1–2 μm during compressions at 1073–1173 K and 10^{-4} to 10^{-2} s^{-1}. In contrast, the mean DRX grain size rapidly increases with an increase in the temperature, especially, at the low strain rate of 10^{-4} s^{-1} (Figure 4a). On the other hand, the rate of increase of DRX subgrain size with an increase in the deformation temperature is much lower as compared with that for DRX grain size, irrespective of the strain rate (Figure 4b).
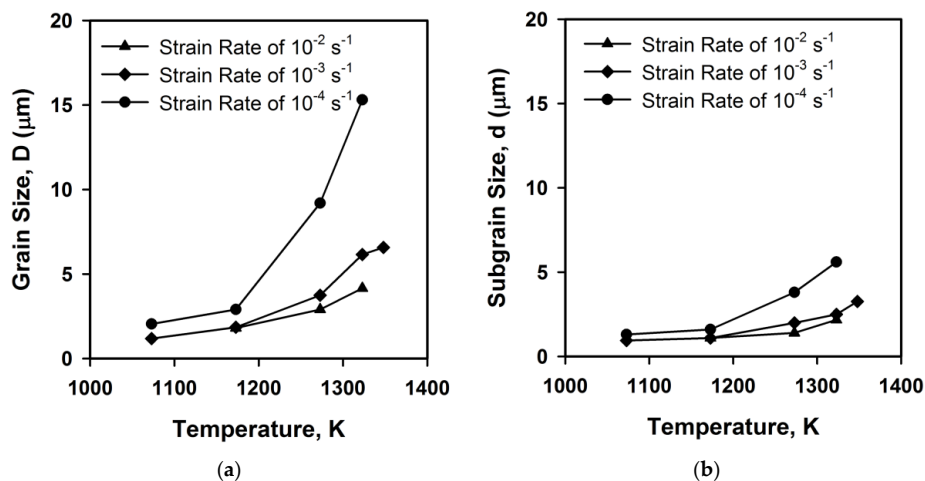
Figure 4. DRX grain (**a**) and subgrain (**b**) size that evolved in the high-nitrogen austenitic stainless steel during compression at different temperatures and strain rates.

The distributions of the DRX grain boundary misorientations that developed in the samples subjected to compressions at a strain rate of 10^{-3} s^{-1} are shown in Figure 5. These developed at different temperatures, and the DRX misorientation distributions are quite similar in appearance and, qualitatively, can be represented as a superposition of three characteristic misorientations. Namely, low-angle misorientations typical of deformation subboundaries, random misorientations (Mackenzie [23]) with a broad peak at 45°, and a sharp peak at 60° corresponding to annealing twins. The changes in the misorientation distributions after compression at different temperatures are mainly associated with the changes in the fractions of low-angle subboundaries and 60° twin boundaries. The peak below 15°, corresponding to low-angle boundaries, sharpens and rises with an increase in the deformation temperature. The twin-related peak against 60° demonstrates the same behavior. After compression at 1073 K, the fraction of 60° misorientations is about 0.05. Increasing the deformation temperature promotes the annealing twin formation. As a result, the fraction of 60° misorientations exceeds 0.15 in the sample compressed at 1323 K. The relative changes in the fractions of 60° misorientations are clearly correlated with the relative changes in the grain/subgrain sizes. The smallest fraction of 60° misorientations corresponds to the sample compressed at 1073 K, in which the grain and subgrains sizes are almost the same.

It has been shown that the steady-state size of DRX grains can be expressed by a power-law function of the flow stress [10,11,24,25]. The relationships between the flow stresses normalized by shear modulus and the sizes of DRX grains and subgrains developed in the present steel during compressions at various temperatures and strain rates are presented in Figure 6. The flow stresses can be related to the DRX grain size through a power-law function with a grain size exponent of −0.76. Such a grain size exponent is typical of discontinuous DRX under hot working conditions [26,27]. On the other hand, the subgrain size is expressed by a different power law function of the flow stress with a size exponent of −1. Therefore, the size difference between DRX grains and subgrains diminishes with increasing flow stress.
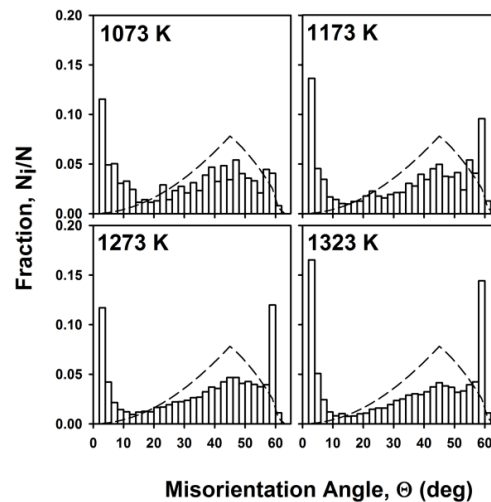
Figure 5. Distributions of the DRX grain boundary misorientations developed in the high-nitrogen austenitic stainless steel during compression to a strain of 1.2 at the indicated temperatures and a strain rate of 10^{-3} s^{-1}. The dashed lines indicate random (Mackenzie) distribution.
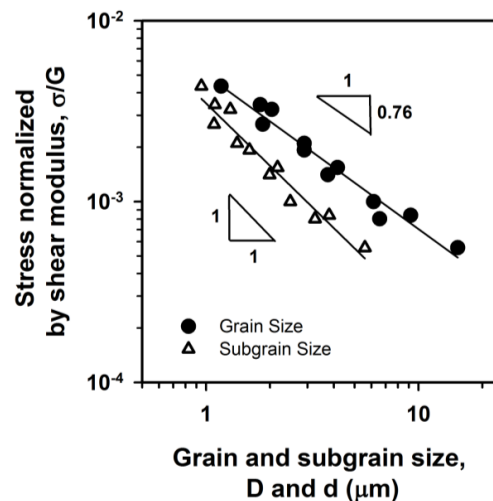
Figure 6. Relationship between the flow stress normalized by the shear modulus (σ/G) and the DRX grain size (D) and subgrain size (d) for the high-nitrogen austenitic stainless steel.

The flow stress and the DRX grain/subgrain sizes are sensitively dependent on the processing conditions [11,28]. Figure 7 shows the relationship between the DRX grain and subgrain sizes and the deformation conditions, which are represented by the temperature-compensated strain rate, Z. The latter was estimated with an activation energy of 280 kJ·mol^{-1} [29]. Increasing Z, generally, leads

to a decrease of both the grain and subgrain sizes. In the range of $Z < 10^{11}$ s^{-1}, corresponding to hot working conditions, the microstructural evolution during deformation of chromium-nickel austenitic stainless steels has been suggested as being associated with the development of discontinuous DRX, when the DRX grain and subgrain sizes exhibit rather strong temperature and/or strain rate dependencies [11]. The DRX grain and subgrain sizes that develop in the present steel can be expressed as $D \sim Z^{-0.27}$ and $d \sim Z^{-0.2}$, respectively. These dependencies predict a certain change in the fraction of ordinary grain boundaries in the DRX microstructures with a change in deformation conditions.
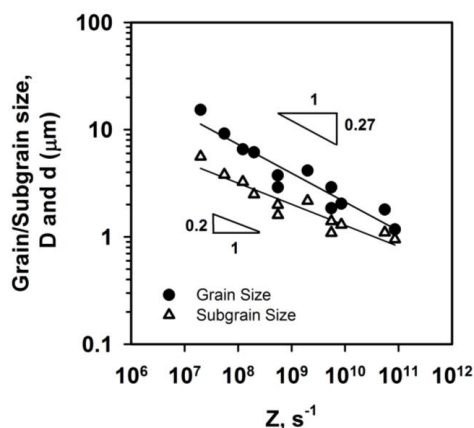
Figure 7. Dependences of the DRX grain/subgrain sizes on the temperature-compensated strain rate (Z) for the high nitrogen austenitic stainless steel.

The fractions of ordinary high-angle grain boundaries and twin-related $\Sigma 3^n$ CSL boundaries in the DRX microstructures that develop in the present steel during hot working are shown in Figure 8. The fraction of ordinary grain boundaries decreases from approx. 0.7 to 0.5 with a decrease in Z from 10^{11} s^{-1} to 10^7 s^{-1}. That is to say, the fraction of high-angle grain boundaries in the DRX microstructures should decrease with an increase in deformation temperature and/or a decrease in strain rate. Such behavior is directly related to the variations of the DRX grain/subgrain sizes with deformation conditions. The difference between the DRX grain size and subgrain size markedly increases with a decrease in Z (Figure 7) or flow stress (Figure 6), then, the fraction of grain boundaries decreases as a ratio of d/D. On the other hand, a decrease in Z (i.e., an increase in deformation temperature and/or a decrease in strain rate) results in an increase in the fraction of $\Sigma 3^n$ CSL boundaries (Figure 8). Thus, the larger DRX grain size corresponds to the larger fraction of twin-related boundaries.
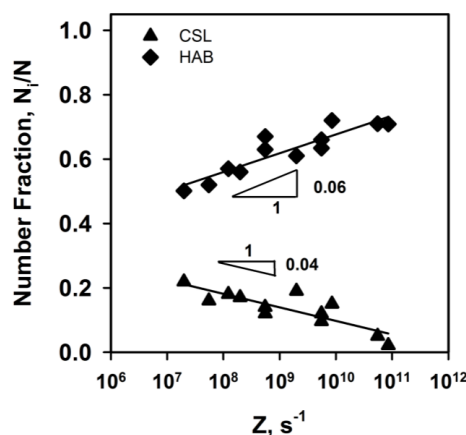
Figure 8. Dependences of the fractions of HAB and CSL boundaries on the temperature-compensated strain rate (Z) for the high-nitrogen austenitic stainless steel.

4. Discussion

Annealing twins have been suggested to appear by growth accidents of a migrating boundary during recrystallization and grain growth [13,18]. Considering an increase in the grain size from D_0 to D the following relationships between the grain size ratio (D/D_0) and the fraction of twin-related $\Sigma 3^n$ CSL boundaries (F_{CSL}) were obtained [20].

$$F_{CSL} = \frac{N_{CSL_0} + K\ln\frac{D}{D_0}}{N_{CSL_0} + K\ln\frac{D}{D_0} + 1} \tag{1}$$

$$N_{CSL_0} = \left(\frac{1}{F_{CSL_0}} - 1\right)^{-1} \tag{2}$$

where N_{CSL0} and F_{CSL0} are the number and fraction of $\Sigma 3^n$ CSL boundaries in the initial microstructure just before the grain growth, respectively, and the numerical factor of $K{\sim}0.5$ depends on the probability of twin formation by a growth accident.

According to the common representation of the discontinuous DRX mechanism, the grain boundary bulging creates a DRX nucleus, which is actually a subgrain that locates under the bulge and almost free of lattice dislocation. Then, this DRX nucleus rapidly grows out and becomes a new grain replacing other pre-existing work-hardened grains [2,3]. Therefore, the size of deformation subgrains can be roughly considered as the starting grain size (D_0), while considering the grain coarsening during discontinuous DRX. Then, the fraction of $\Sigma 3^n$ CSL boundaries can be evaluated by Equation (1), taking $D_0 = d$ for the present DRX microstructures that developed under various deformation conditions.

Figure 9 shows the relationship between F_{CSL} and D/d that were obtained for austenitic stainless steels in the present (filled symbols) and previous (open symbols) studies [20,30] as well as that calculated by Equation (1) with $K = 0.5$ (solid line). It should be noted that previous studies dealt with continuous post-dynamic recrystallization after large strain deformation by multiple warm forgings at different temperatures, whereas the present study considers conventional DRX microstructures.
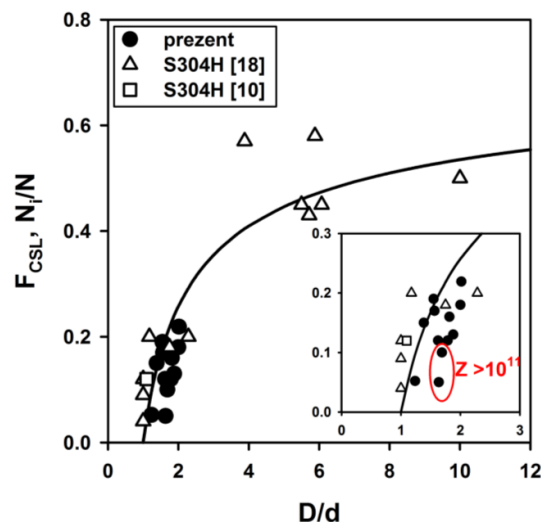
Figure 9. Relationship between the fraction of CSL boundaries (F_{CSL}) and the grain/subgrain size ratio (D/d).

Nevertheless, all data points in Figure 9 locate quite near the position predicted by Equation (1), suggesting that the fraction of $\Sigma 3^n$ CSL boundaries can be expressed by a unique function of the grain size change irrespective of the grain coarsening mechanisms. Some data points to the right of the curve (s. insert in Figure 9) were obtained under conditions of $Z > 10^{11}$ s^{-1}, when the contribution of

discontinuous DRX to the new grain development becomes small, i.e., new grains develop without remarkable grain growth [11].

Let us consider the effect of deformation conditions from cold to hot working on the grain boundary assemblies evolved after sufficiently large strains, i.e., under conditions of apparent steady state deformation. The change in the fraction of ordinary high-angle boundaries (F_{HAB}) in Figure 9 clearly correlates with the change in subgrain/grain size ratio (d/D) in Figures 7 and 8. The hot deformation conditions selected in the present study correspond to the range of discontinuous DRX. Therefore, the fraction of ordinary grain boundaries in discontinuous DRX microstructures decreases with a decrease in Z (increase in temperature and/or decrease in strain rate). In a previous paper, a three-stage relationship between flow stress and dynamic grain size has been suggested for a wide temperature interval [31,32]. Three power law functions with different grain size exponents of about -0.7, -0.3, and -1.0 have been reported for discontinuous DRX during hot working, continuous DRX during warm working, and grain refinement during cold working. On the other hand, the subgrain size can be related to the flow stress with a size exponent of -1.0 in the whole temperature range. Such dependences suggest a three-stage variation of boundary characteristics on the processing conditions, as schematically shown in Figure 10.

A decrease in the deformation temperature corresponds to the sequential change from hot working to warm working and then to cold working (the regions of I to II to III in Figure 10). The fraction of ordinary high-angle grain boundaries increases as the deformation temperature decreases within the conditions of hot working (region I). Correspondingly, slow down grain growth with decreasing temperature results in a gradual decrease in the fraction of $\Sigma 3^n$ CSL boundaries. The transition to warm working is accompanied by a change in the grain size dependence on deformation conditions/flow stress. The grain size that evolves at sufficiently large strains rapidly approaches the subgrain size, i.e., $D/d \rightarrow 1$, as the deformation temperature decreases. Therefore, the fraction of high-angle grain boundaries comes close to 1, while F_{CSL} becomes negligibly small (region II in Figure 10). A further decrease in the deformation temperature to cold working leads to the cessation of the grain growth. The ultrafine grains that develop under conditions of severe plastic deformation are entirely bounded by high-angle boundaries [33,34], leading to $F_{HAB}\sim 1$. The $\Sigma 3^n$ CSL boundaries may appear during severe plastic deformation as result of deformation twinning, but this is not an annealing phenomenon.
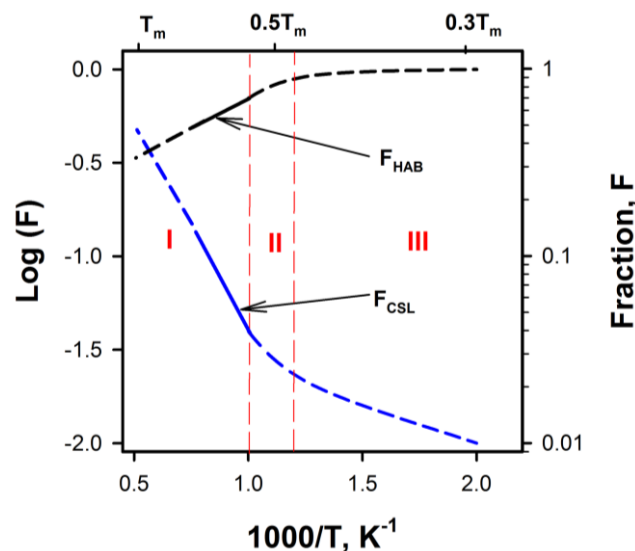
Figure 10. Variations of the fractions of HAB (F_{HAB}) and CSL (F_{CSL}) boundaries in austenitic stainless steels with deformation conditions.

5. Conclusions

The deformation microstructures that developed in a high-nitrogen austenitic stainless steel during hot working accompanied by dynamic recrystallization (DRX) were studied. The main results can be summarized as follows:

1. The relationship between the DRX grain/subgrain size and flow stress can be expressed by power-law functions with different size exponents of -0.76 (grains) and -1.0 (subgrains), which is typical of discontinuous DRX under hot working conditions. Correspondingly, power-law functions with exponents of -0.27 and -0.2 are held for the effect of temperature-compensated strain rate (Z) on the grain and subgrain sizes, respectively.

2. The fraction of ordinary high-angle boundaries in DRX microstructures increases from approx. 0.5 to 0.7, while the fraction of twin-related $\Sigma 3^n$ CSL boundaries decreases from 0.25 to 0.05 as Z increases from 10^7 s^{-1} to 10^{11} s^{-1}. Both the fraction of ordinary grain boundaries and the fraction of $\Sigma 3^n$ CSL boundaries depend on the grain and subgrain sizes, i.e., D and d, and can be expressed by functions of the ratio of D/d.

Author Contributions: The present paper is a result of fruitful collaboration of all co-authors. R. Kaibyshev designed the research theme; A. Belyakov and M. Tikhonova selected the experimental procedure; P. Dolzhenko carried out the experimental study. Then, all co-authors discussed and analyzed the obtained results.

Conflicts of Interest: The authors declare no conflict of interest.

References

1. Sakai, T.; Jonas, J.J. Dynamic recrystallization: Mechanical and microstructural considerations. *Acta Metall.* **1984**, *32*, 189–209. [CrossRef]

2. Sakai, T.; Belyakov, A.; Kaibyshev, R.; Miura, H.; Jonas, J.J. Dynamic and post-dynamic recrystallization under hot, cold and severe plastic deformation conditions. *Prog. Mater. Sci.* **2014**, *60*, 130–207. [CrossRef]

3. Humphreys, F.J.; Hatherly, M. *Recrystallization and Related Annealing Phenomena*; Elsevier Science: New York, NY, USA, 2004.

4. Huang, K.; Logé, R.E. A review of dynamic recrystallization phenomena in metallic materials. *Mater. Des.* **2016**, *111*, 548–574. [CrossRef]

5. McQueen, H.J.; Jonas, J.J. Recovery and Recrystallization during High Temperature Deformation. In *Treatise on Materials Science and Technology*; Arsenault, R.J., Ed.; Academic Press: New York, NY, USA, 1975; Volume 6, pp. 394–493.

6. Maki, T.; Akasaka, K.; Okuno, K.; Tamura, I. Dnamic recrystallization of austenite in 18-8 stainless steel and 18 Ni maraging steel. *Trans. Iron Steel Inst. Jpn.* **1982**, *22*, 253–261. [CrossRef]

7. Belyakov, A.; Sakai, T.; Miura, H.; Kaibyshev, R. Grain refinement under multiple warm deformation in 304 type austenitic stainless steel. *ISIJ Int.* **1999**, *39*, 592–599. [CrossRef]

8. Sakai, T. Dynamic recrystallization microstrustures under hot working conditions. *J. Mater. Process. Technol.* **1995**, *53*, 349–361. [CrossRef]

9. Belyakov, A.; Tikhonova, M.; Yanushkevich, Z.; Kaibyshev, R. Regularities of grain refinement in an austenitic stainless steel during multiple warm working. *Mater. Sci. Forum* **2013**, *753*, 411–416. [CrossRef]

10. Dudova, N.; Belyakov, A.; Sakai, T.; Kaibyshev, R. Dynamic recrystallization mechanisms operating in a Ni-20%Cr alloy under hot-to-warm working. *Acta Mater.* **2010**, *58*, 3624–3632. [CrossRef]

11. Tikhonova, M.; Belyakov, A.; Kaibyshev, R. Strain-induced grain evolution in an austenitic stainless steel under warm multiple forging. *Mater. Sci. Eng. A* **2013**, *564*, 413–422. [CrossRef]

12. Wang, X.; Brunger, E.; Gottstein, G. The role of twinning during dynamic recrystallization in alloy 800 H. *Scr. Mater.* **2002**, *46*, 875–880. [CrossRef]

13. Mahajan, S. Critique of mechanisms of formation of deformation, annealing and growth twins: Face-centered cubic metals and alloys. *Scr. Mater.* **2013**, *68*, 95–99. [CrossRef]

14. Watanabe, T. Approach to Grain Boundary Design for Strong and Ductile Polycrystals. *Res. Mech.* **1984**, *11*, 47–84.

15. Randle, V. Twinning-related grain boundary engineering. *Acta Mater.* **2004**, *52*, 4067–4081. [CrossRef]

16. Fang, X.; Liu, Z.; Tikhonova, M.; Belyakov, A.; Wang, W. Evolution of texture and development of $\Sigma 3^n$ grain clusters in 316 austenitic stainless steel during thermal mechanical processing. *J. Mater. Sci.* **2013**, *48*, 997–1004. [CrossRef]

17. Cahoon, J.R.; Qiangyong, L.I.; Richards, N.L. Microstructural and processing factors influencing the formation of annealing twins. *Mater. Sci. Eng. A* **2009**, *526*, 56–61. [CrossRef]

18. Pande, C.S.; Imam, M.A.; Rath, B.B. Study of Annealing Twins in FCC Metals and Alloys. *Metall. Trans. A* **1990**, *21*, 2891–2896. [CrossRef]

19. Pande, C.S.; Imam, M.A. Grain growth and twin formation in boron-doped nickel polycrystals. *Mater. Sci. Eng. A* **2009**, *512*, 82–86. [CrossRef]

20. Tikhonova, M.; Kuzminova, Y.; Fang, X.; Wang, W.; Kaibyshev, R.; Belyakov, A. $\Sigma 3$ CSL boundary distributions in an austenitic stainless steel subjected to multidirectional forging followed by annealing. *Philos. Mag.* **2014**, *94*, 4181–4196. [CrossRef]

21. Jonas, J.J.; Sellars, C.M.; Tegart, W.J. Strength and structure under hot-working conditions. *Metall. Rev.* **1969**, *130*, 1–33. [CrossRef]

22. Belyakov, A.; Miura, H.; Sakai, T. Dynamic recrystallization under warm deformation of a 304 type austenitic stainless steel. *Mater. Sci. Eng. A* **1998**, *255*, 139–147. [CrossRef]

23. Mackenzie, J.K. Second Paper on the Statistics Associated with the Random Disorientation of Cubes. *Biometrika* **1958**, *45*, 229–240. [CrossRef]

24. Derby, B. The Dependence of Grain Size on Stress during Dynamic Recrystallization. *Acta Metall. Mater.* **1991**, *39*, 955–962. [CrossRef]

25. Belyakov, A.; Gao, W.; Miura, H.; Sakai, T. Strain induced grain evolution in polycrystalline copper during warm deformation. *Metall. Mater. Trans. A* **1998**, *29*, 2957–2965. [CrossRef]

26. Beladi, H.; Cizek, P.; Hodgson, P.D. On the Characteristics of Substructure Development through Dynamic Recrystallization. *Metall. Mater. Trans. A* **2009**, *40*, 1175–1189. [CrossRef]

27. Cizek, P. The microstructure evolution and softening processes during high-temperature deformation of a 21Cr-10Ni-3Mo duplex stainless steel. *Acta Mater.* **2016**, *106*, 129–143. [CrossRef]

28. Abson, D.J.; Jonas, J.J. Substructure strengthening in zirconium and zirconium-tin alloys. *J. Nucl. Mater.* **1972**, *42*, 73–85. [CrossRef]

29. Frost, H.J.; Ashby, M.F. *Deformation Echanism Maps*; Pergamon press: Oxford, UK, 1982.

30. Tikhonova, M.; Kaibyshev, R.; Fang, X.; Wang, W.; Belyakov, A. Grain boundary assembles developed in an austenitic stainless steel during large strain warm working. *Mater. Charact.* **2012**, *70*, 14–20. [CrossRef]

31. Tikhonova, M.; Enikeev, N.; Valiev, R.Z.; Belyakov, A.; Kaibyshev, R. Submicrocrystalline Austenitic Stainless Steel Processed by Cold or Warm High Pressure Torsion. *Mater. Sci. Forum* **2016**, *838–839*, 398–403. [CrossRef]

32. Belyakov, A.; Zherebtsov, S.; Salishchev, G. Three-stage relationship between flow stress and dynamic grain size in titanium in a wide temperature interval. *Mater. Sci. Eng. A* **2015**, *628*, 104–109. [CrossRef]

33. Humphreys, F.J.; Prangnell, P.B.; Bowen, J.R.; Gholinia, A.; Harris, C. Developing Stable Fine-Grain Microstructures by Large Strain Deformation. *Philos. Trans. R. Soc. Lond. A* **1999**, *357*, 1663–1681. [CrossRef]

34. Valiev, R.Z.; Langdon, T.G. Principles of equal-channel angular pressing as a processing tool for grain refinement. *Prog. Mater. Sci.* **2006**, *51*, 881–981. [CrossRef]